INL/EXT-15-35033

Particle Size and Shape Distributions of Hammer Milled Pine

Tyler Westover
Austin Matthews
Luke Williams
Chad Ryan

April 2015

The INL is a U.S. Department of Energy National Laboratory
operated by Battelle Energy Alliance

INL/EXT-15-35033

Particle Size and Shape Distributions of Hammer Milled Pine

Tyler Westover
Austin Matthews
Luke Williams
Chad Ryan

April 2015

Idaho National Laboratory
Idaho Falls, Idaho 83415

http://www.inl.gov

Prepared for the
U.S. Department of Energy
Assistant Secretary for Energy Efficiency and Renewable Energy
Under DOE Idaho Operations Office
Contract DE-AC07-05ID14517

Report Title: Particle size and shape distributions of hammer milled pine INL/EXT-15-35033
Project Title: Computational Pyrolysis Consortium – INL (2.5.1.304)
Award Number: 16932
Recipient: INL
Project Location: INL
Reporting Period: FY15 Q1
Written by: Tyler Westover, Austin Matthews.
Participating Researchers: Luke Williams, Chad Ryan

Milestone: Measure size and shape distributions for a material at two grind sizes that are relevant for fast pyrolysis, such as hammer mill grinding using 6 mm and 4 mm screens

INTRODUCTION

Particle size and shape distributions impact particle heating rates and diffusion of volatized gases out of particles during fast pyrolysis conversion, and consequently must be modeled accurately in order for computational pyrolysis models to produce reliable results for bulk solid materials. For this milestone, lodge pole pine chips were ground using a Thomas-Wiley #4 mill using two screen sizes in order to produce two representative materials that are suitable for fast pyrolysis. For the first material, a 6 mm screen was employed in the mill and for the second material a 3 mm screen was employed in the mill. Both materials were subjected to RoTap sieve analysis, and the distributions of the particle sizes and shapes were determined using digital image analysis. The results of the physical analysis will be fed into computational pyrolysis simulations to create models of materials with realistic particle size and shape distributions. This milestone was met on schedule.

METHODS

Sieve particle classification

Sieve classification of the materials was performed in triplicate according to ASAE S319.3 using a standard Ro-tap separator. The cumulative particle passing distributions (CPDs) and the associated probability density distributions (PDDs), which represent the derivative of the CPDs, were calculated. For all of the analyses, the 50% cumulative passing percentile sieve size, t_{50}, was calculated by interpolation to find the theoretical sieve size that corresponds to retaining 50% of the particles by mass. This sieve size corresponds to the 50% height on the CPD. Similarly, the 16% and 84% cumulative passing percentile sieve sizes (t_{16} and t_{84}, respectively) were also calculated in order to determine the ranges of the particle size distributions.

Digital image analysis

After particle separation using sieve analysis, all particles that were retained on a 0.6 mm and larger sieves were subjected to digital image analysis to determine the size and shape properties of all particles with diameters larger than approximately 0.6 mm. A Clemex digital image analysis system (Clemex Technologies Inc., QC, Canada) at 48X magnification was used to perform the digital image analysis. The materials were also sieved using 1.4, 0.85, and 0.425 mm sieves, and the material retained on each sieve was also subjected to particle size and shape distribution analysis.

Digital image analysis was performed by sparsely sprinkling representative samples onto a moving conveyor belt, which was positioned approximately 1 meter below a digital camera (Clemex L 1.4 C CCD: 1392 x 1024 pixels). Approximately fifty images were collected of each replicate for a mean

number of particles per analysis greater than 4,000. The particles and the background are separated in the software through a grey threshold. The software also allows particles with certain roughness values (ratio of convex perimeter to actual perimeter) to be excluded from the measurement, and this feature was employed to prevent overlapping particles from skewing the measurements. Each set of images was analyzed cumulatively using the following parameters:

- Aspect ratio (*aspect*): ratio of length over width (longest ferret to shortest ferret);
- Feret: distance between two parallel tangents on each side of a particle (analogous to using a caliper) measured at a specific angle with respect to the process frame;
- Length (*l*): longest of 32 ferets every 5.625° measured for each object;
- Width (*w*): shortest of 32 ferets every 5.625° measured for each object;
- Main Length (*ml*): the measure of the longest feret perpendicular to the shortest ferret;
- Perimeter (*p*): objects perimeter interpolated from three points;
- Roughness (*rough*): ratio of convex perimeter to perimeter; provides a measure of the jaggedness of an object's edges;
- Roundness (*round*): a shape measure that quantifies the "roundness" of an object's edges.
  $round = (4 \cdot \text{Area})/(\pi \cdot L \cdot L)$;
- Sphericity (*sphere*): compares the perimeter of an object to that of a sphere:
  $sphere = (4 \cdot \pi \cdot \text{Area})/[\text{Perimeter}]^2$.

The digital imaging method was applied separately to 20 particles with lengths in the range of 1.7 to 2.4 mm (see Fig. 1A). The maximum lengths, widths, and depths of these particles were determined by hand using a digital caliper and manual image analysis, and their masses were determined using a 5 digit mass scale. The digital imaging method was also applied separately to a set of white rectangles and ovals printed on black paper. The rectangle and oval shapes were printed to have lengths and widths that closely matched those of the 20 particles that were measured by hand (Fig. 1B and C). Additional sets of white rectangles were also analyzed that had lengths and widths that were 2X (Fig. 1D), 0.5X (Fig. 1E), and 0.25X (Fig. 1F) those of the first set of rectangles in order to determine the accuracy of the digital method for particles of different sizes.

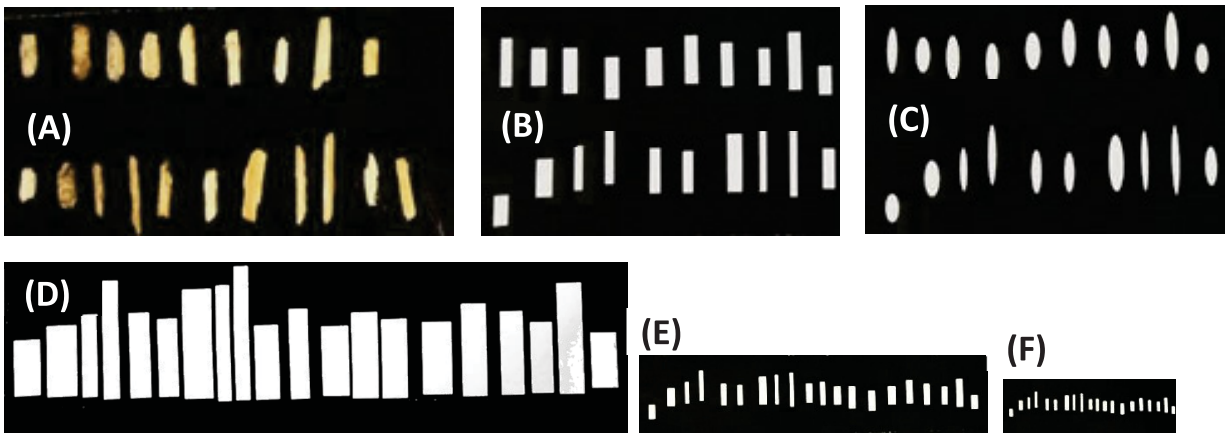

Figure 1. Particles and shapes used to validate digital imaging method. (A) Reference particles; (B) and (C) rectangles and ovals, respectively, with lengths and widths that match validation particles; (D), (E) and (F) show rectangles with lengths and widths that are 2X, 0.5X and 0.25X those of the reference particles.

RESULTS

Figure 2 compares dimensions measured manually with those measured by the camera for the 20 reference particles and also for the similarly sized rectangles and the rectangles at 0.25X scale. The results show good agreement, although the dimensions measured by the digital camera are consistently 470 microns larger than those obtained from manual measurements. All results from the digital camera presented in subsequent figures and tables have been scaled to bring the camera measurements into agreement with those obtained manually.

Figure 3 displays the cumulative particle passing distributions (CPDs) of the 20 reference particles that were used to verify the digital imaging method. The solid black squares and solid blue triangles show CPDs of the particles based upon measured mass and estimated block volume ($L \cdot W \cdot D$), respectively, as functions of particle length as measured manually. The solid red circles show the CPD of the particles based upon the estimated particle block volume ($ml \cdot w \cdot w$) as measured using the automated Clemex software as function of particle width. Parameters written in upper case font were measured manually, whereas parameters measured using automated software are reported in lower case font. The measured CPDs based upon particle length show good agreement whether they are based upon particle mass or upon estimated particle block volume for measurements collected manually or using the digital software. Hollow symbols corresponding to the solid symbols exhibit measured CPDs as functions of measured particle volume. Good agreement is again obtained between measurements based upon mass and estimated particle block volume, although results from the camera do exhibit some deviation for particles smaller than approximately 1.5 mm.

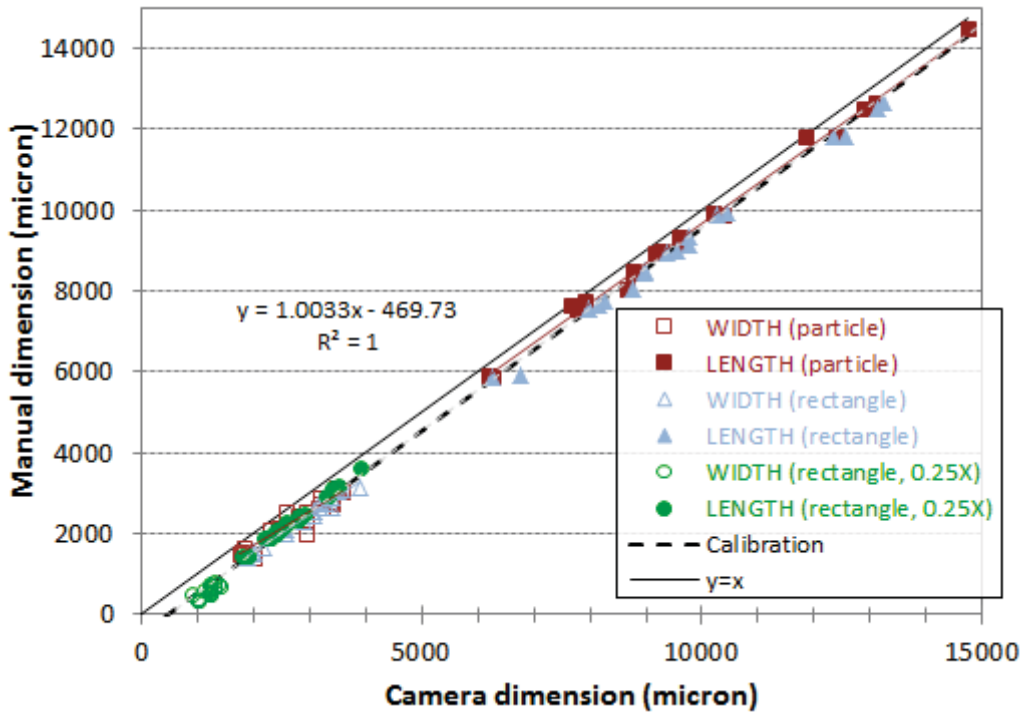

Figure 2. Particles and shape dimensions as measured manually and also as measured using a digital camera.

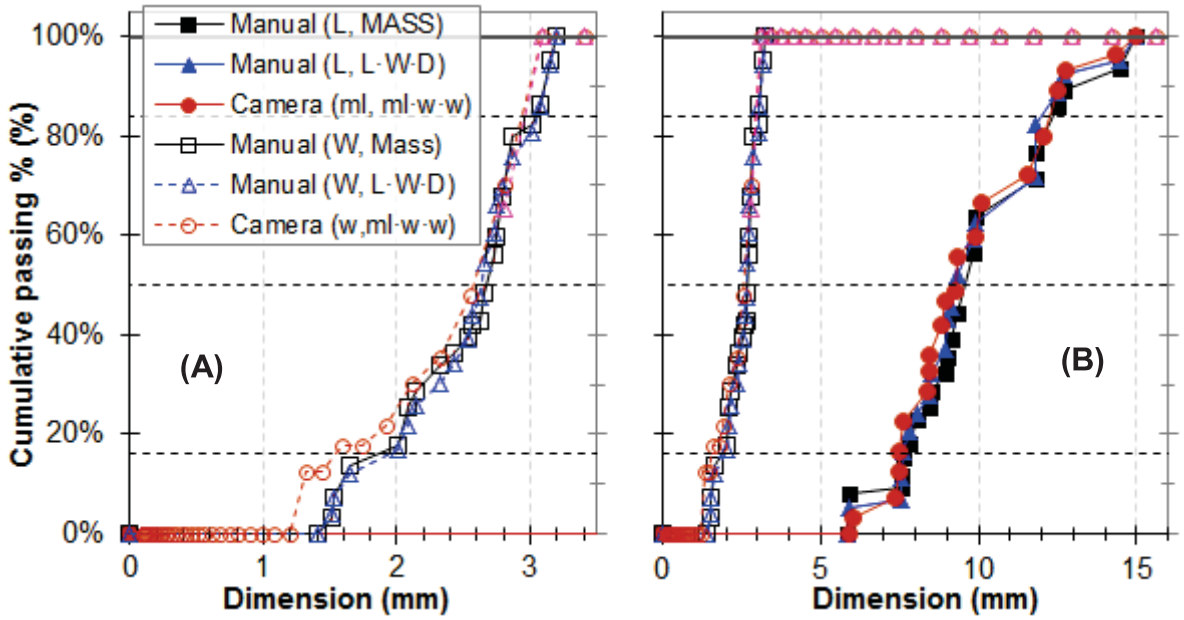

Figure 3. Cumulative particle passing distributions (CPDs) of the 20 reference particles featured in Fig. 1. CPDs plotted as functions of particle length and width are shown as solid and hollow symbols, respectively. CPDs based upon particle mass are shown as squares, while those based upon estimated particle block volumes are shown as triangles and circles. Panels (A) and (B) are similar except that (B) shows a larger scale.

Figure 4 shows CPDs of lodge pole pine samples ground with 3 mm and 6 mm screens and then sieved with a 0.60 mm screen to remove fine particles. CPDs were measured with a digital camera and are based upon estimated block volume and are expressed as functions of particle length and width, which are shown as solid and hollow symbols, respectively. CPDs based upon particle sieve analysis (mass) are shown as X's. Panels (A) and (B) are similar except that (B) shows a larger scale. Uncertainty bars show standard deviation of replicates from three separate representative samples. An average of over 4,000 particles were analyzed for each replicate. Notably, the CPDs based upon sieve analysis are similar to those obtained using the digital camera as functions of particle width.

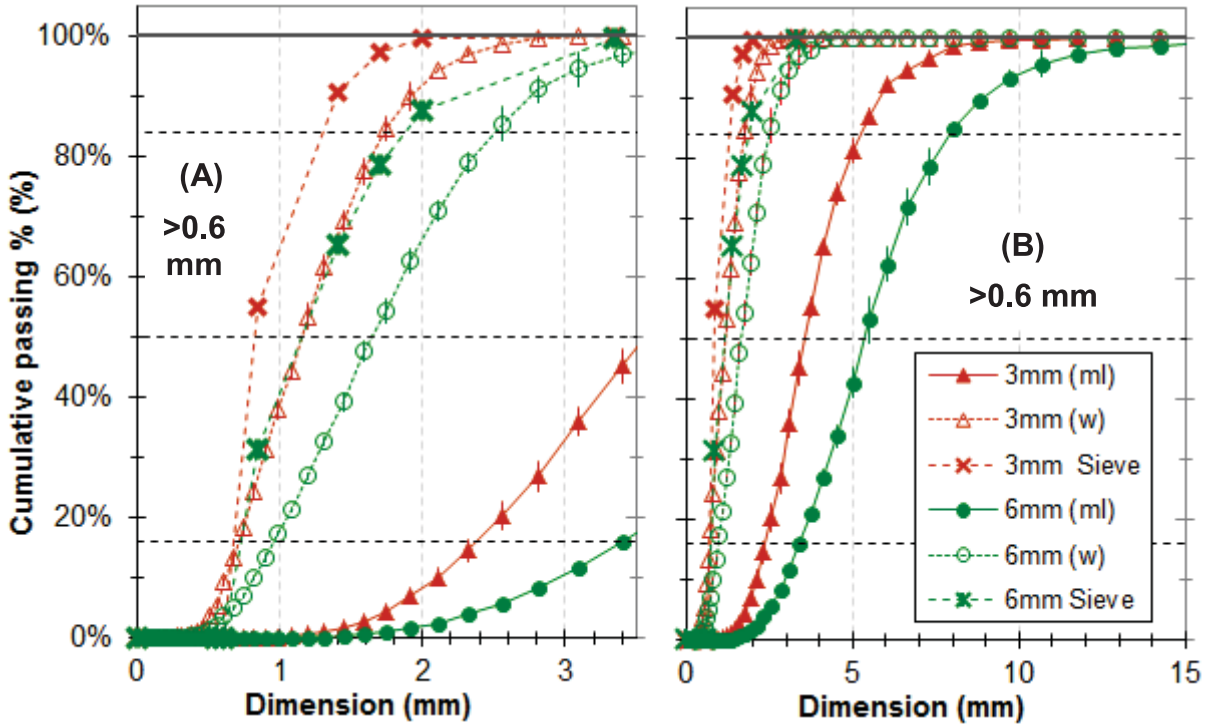

Figure 4. Cumulative particle passing distributions (CPDs) of lodge pole pine samples ground with 3 mm and 6 mm screens and then sieved with a 0.60 mm screen to remove fine particles. CPDs as functions of particle length and width are shown as solid and hollow symbols, respectively. CPDs based upon particle sieve analysis are shown as X's. Panels (A) and (B) are similar except that (B) shows a larger scale. Uncertainty bars show standard deviation of replicates from three separate representative samples.

Figure 5 shows cumulative particle passing distributions (CPDs) of the same lodge pole pine samples ground with 3 mm and 6 mm screens and then sieved with a 1.4, 0.85, and 0.425 mm sieves. CPDs of roundness and aspect ratio are shown for each sieve fraction. The largest particles from the 3 mm grind appear to be the most round and the largest particles from the 6 mm grind are the next most round. Not surprisingly, the largest particles also have the lowest aspect ratios. The other fractions appear to have similar roundness and aspect ratios, except for the 3 mm middle grind fraction, which has a relatively high aspect ratio and low roundness. Table 1 summarizes the mass percentages, size and shape information for the material fractions separated from the 3 mm and 6 mm loblolly pine grinds.

The results of these physical analyses will be employed in computational pyrolysis simulations to create models of materials with realistic particle size and shape distributions.

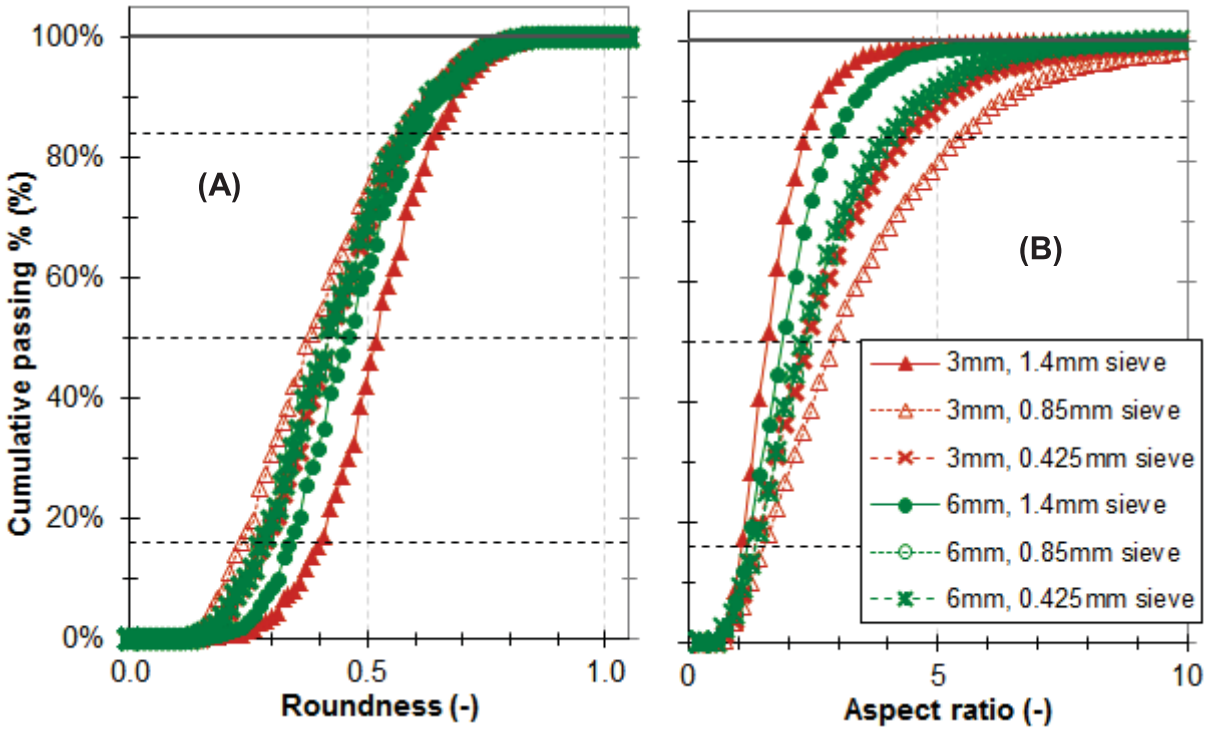

Figure 5. Cumulative particle passing distributions (CPDs) of lodge pole pine samples ground with 3 mm and 6 mm screens and then sieved with a 1.4, 0.85, and 0.425 mm sieves. CPDs of roundness and aspect ratio are shown for each sieve fraction. CPDs were measured with a digital camera and are based upon estimated block volume.

Table 1. Mass percentages, size and shape information for the material fractions separated from the 3 mm and 6 mm grinds.

Material	Mass	w_{50}	w_{84}	ml_{50}	ml_{84}	$round_{50}$	$aspect_{50}$
(-)	(%)	(mm)	(mm)	(mm)	(mm)	(-)	(-)
3 mm, >0.6 mm	58	1.15	1.69	3.50	5.09	0.42	2.94
3 mm, 1.4 mm sieve	4.8	2.1	2.6	4.46	5.93	0.52	1.6
3 mm, 0.85 mm sieve	21.3	0.93	1.3	3.12	5.44	0.38	2.9
3 mm, 0.425 mm sieve	36.7	0.95	1.5	2.89	4.39	0.37	2.4
6 mm, >0.6 mm	74%	1.61	2.44	5.18	7.76	0.35	3.22
6 mm 1.4 mm sieve	27.7	2.4	3.2	5.98	8.30	0.46	1.9
6 mm, 0.85 mm sieve	26.9	1.60	2.07	4.52	6.84	0.42	2.4
6 mm, 0.425 mm sieve	14.7	0.95	1.51	3.14	4.89	0.40	2.6

w_{50} = median *width*; w_{84} = 84th percentile of *width*; ml_{50} median *main length*; ml_{84} = 84th percentile of *main length*; $round_{50}$ = median *roundness*; $aspect_{50}$ = median *aspect ratio*.